Journal of King Saud University – Science 34 (2022) 102047

Contents lists available at ScienceDirect

Journal of King Saud University – Science

journal homepage: www.sciencedirect.com

Original article

Facile green synthesis of semiconductive ZnO nanoparticles for photocatalytic degradation of dyes from the textile industry: A kinetic approach

Jayachamarajapura Pranesh Shubha [a,*], Kiran Kavalli [b], Syed Farooq Adil [c,*], Mohamed E. Assal [c], Mohammad Rafe Hatshan [c], Narsimhaswamy Dubasi [d]

[a] Department of Chemistry, Don Bosco Institute of Technology, Mysore Road, Bangalore 560074, India
[b] Department of Mechanical and Automobile Engineering, School of Engineering and Technology, CHRIST University, Bangalore 560074, India
[c] Department of Chemistry, College of Science, King Saud University, P.O. Box 2455, Riyadh 11451, Saudi Arabia
[d] 12001 Belcher Rd S, Apt N226, Largo, FL 33773-5039, USA

ARTICLE INFO

Article history:
Received 16 January 2022
Revised 16 April 2022
Accepted 17 April 2022
Available online 22 April 2022

Keywords:
ZnO
Methylene blue
Alizarin red S
Degradation
Photocatalysis

ABSTRACT

One-pot, facile and green synthesis of zinc oxide nanoparticles are synthesized using cow dung as fuel by combustion procedure. The synthesized material is characterized by using various techniques such as XRD, FTIR, UV, FESEM, and EDX. To assess the photocatalytic efficacy of the as-synthesized material, harmful cationic and anionic dyes such as methylene blue (MB) and alizarin red S (AZ) dyes, respectively, are selected as benchmark dyes. The influence of light source, dye concentration, photocatalyst dosage, and pH value on the efficiency of photocatalyst and kinetics of photodegradation are systematically studied. The photodegradation results revealed that the synthesized ZnO NPs exhibited removal efficiency of MB and AZ dyes upon irradiation with UV light. Concisely, the removal efficacy of the ZnO NPs under UV light irradiation exhibited an MB and AZ degradation of 99.9% and 96.8%, respectively. A reasonable photo-catalytic mechanism for the high photodegradation efficacy of MB and AZ dyes by the prepared photocatalyst is also proposed. The green fabricated photocatalyst is promising material and could be applied for waste-water remediation and other ecological applications.

1. Introduction

In recent years, the harmful organic pigments and their wastewater products generated from various industries such as textile, plastic, paper, pesticides, leather, and petrochemical industries were severely contaminating aquatic life and poisoning human beings (Maruthupandy et al., 2020). These toxic organic dyes cause severe environmental pollution and approximately 10–15% of the dyes are produced in the wastewater which is a fundamental source of environmental pollution (Koutavarapu et al., 2020). The organic dyes existent in the effluents produced from the above-mentioned industries are difficult to degrade, owing to their high chemical stabilities. Many physicochemical and biological methods including chemical oxidation, adsorption, precipitation, ion-exchange, biological, reverse osmosis, and photocatalytic processes were applied to degrade the harmful organic dye (Mydeen et al., 2020). However, most of these aforementioned procedures suffer from many limitations such as high cost and inefficacious (Alharthi et al., 2020). Besides, these techniques need a costly operation and recurring expenses, therefore these processes are not suitable for small-scale industry. Hence, effective, low cost and environmentally-friendly alternative procedures are required to reduce the aforementioned disadvantages for the decomposition of dyes present in effluents (Soto-Robles et al., 2021; Subramanian et al., 2022).

Among the processes suggested so far, Advanced-Oxidation-Process (AOP), which is considered as one of the most effective strategies for the decomposition of noxious organic pollutants in water with the use of semiconductor-based photocatalysts, attributed to its high efficacies, environmentally friendliness, and inex-

* Corresponding authors.
E-mail addresses: shubhapranesh@gmail.com (J.P. Shubha), sfadil@ksu.edu.sa (S. F. Adil).
Peer review under responsibility of King Saud University.

Production and hosting by Elsevier

https://doi.org/10.1016/j.jksus.2022.102047
1018-3647/

pensive (Pouretedal et al., 2009; Alharthi et al., 2020). This promising method includes the decomposition of deleterious organic dyes through a mechanism of oxidation by the production of highly reactive free radical ions ($OH^{\cdot}$) due to the presence of a photocatalyst under the influence of light source which could be UV light, visible light, or natural solar light irradiation. Semiconductor materials can decompose the organic and synthetic pigments into harmless and eco-friendly compounds, such as water and carbon dioxide (Natarajan et al., 2018b). The semiconductor-based photocatalysts are highly proficient in decreasing charge reunion which leads to high UV and Vis. light performance owing to their narrow bandgap energy (Natarajan et al., 2018a). Various photocatalysts have been explored worldwide, among the different types of photocatalysts, metal oxides that possess outstanding bandgap energy of 3.32 eV exhibit superb potential in industrial applications (López et al., 2019; Barglik-Chory et al., 2004).

The photocatalytic degradation of dyes includes the generation of positively charged holes (h^+) in the valence band (VB) and negatively charged electrons (e^-) in the conduction band (CB) in presence of light sources such as from UV light or solar irradiation. The photon energy has to be larger than the band-gap of the semiconductor materials utilized as a photocatalyst to excite the electrons from the valence band to the conduction band (Hernández-Carrillo et al., 2018). These photo-induced charge carriers (electrons and holes) are further used for oxidation and reduction of different types of pollutants existent in the wastewater, for example, the MB and AZ dyes (Bhushan et al., 2020). The semiconductor-based photocatalysts including ZnO, CeO_2, ZrO_2, TiO_2, etc., are extensively employed as photocatalysts for the decomposition of organic contaminants (Suresh and Sivasamy 2020). Among the different types of semiconductors, ZnO is a premium photocatalyst and possesses numerous applications in several fields including energy storage devices, cancer therapy, supercapacitors, solar cells, and ecological pollution abatement owing to its unique properties such as non-toxicity, low cost, wide adsorption spectrum, abundant availability, high electron mobility and high thermal/chemical/physical stability (Wetchakun et al., 2019). These aforementioned merits make ZnO an idealistic choice for the photocatalytic degradation of dyes. Despite these advantages, ZnO nanoparticles also have drawbacks including broad band-gap, the photo-induced charge carriers recombination at a rapid rate and hence limits the usage of ZnO (Hernández-Carrillo et al., 2018; Look, 2001).

In this research, an attempt is made to synthesize ZnO NPs as photocatalyst in ecologically friendly and inexpensive combustion methodology using the cow dung as fuel to achieve high photodecomposition activity over two organic chronic dyes (MB and AZ dyes) as demonstrated in Scheme 1. The prepared ZnO NPs are employed as photocatalyst for the removal of dyes in an aqueous solution in presence of various light sources. Additionally, the effect of several catalytic factors such as irradiation time, dye concentration (ppm), photocatalyst amount, and pH value on the photocatalytic decomposition of MB and AZ dyes are investigated. The photocatalytic data disclosed that the ZnO NPs photocatalyst exhibited superior photocatalytic efficiency for the degrading of MB and AZ dyes under UV irradiation, and a 99.9% and 96.8% of MB and AZ dyes are decomposed within 100 min, respectively, under the optimal conditions.

2. Materials and methods

2.1. Materials

Analytical grade zinc nitrate hexahydrate, $Zn(NO_3)_2{\cdot}6H_2O$ (Sigma-Aldrich) is utilized without further purification. Cow dung is collected and dehydrated under sunlight for 15 days and used as fuel.

2.2. Synthesis of ZnO NPs photocatalyst

The calculated amounts of zinc nitrate hexahydrate is dissolved in 10 mL of distilled water and 1.0 g of fresh cow dung with constant vigorous stirring for 30 min. Subsequently, the obtained mixture are kept in a muffle furnace at 400 °C. A pale yellow powder is obtained after 10 min, which is calcined at the same temperature for 3 h.

2.3. Characterizations of ZnO NPs photocatalyst

The specifics related to the characterization instruments are mentioned in the supplementary file.

3. Results and discussion

3.1. Characterization of the ZnO NPs photocatalyst

The UV–visible absorption spectrum of as-fabricated ZnO NPs are presented in Fig. 1(a) with an inset figure of the Tauc plot. The absorption maximum was obtained at 368 nm wavelength indicating the formation of hexagonal ZnO NPs. This is attributed to the fundamental band-gap absorption occurring by the electronic transition between the valence band of the oxygen (2p orbitals) to the conduction band of Zn atoms (3d orbitals) ($O_{2p} \rightarrow Zn_{3d}$) as previously reported (Zak et al., 2011). The direct bandgap energy of as-fabricated ZnO NPs is calculated as 3.19 eV by extrapolating the straight line in the Tauc plot.

To comprehend the crystal structure of the as-fabricated ZnO NPs, the powder XRD spectroscopic analysis is employed. Fig. 1 (b) illustrates the XRD diffractogram for the ZnO NPs obtained by eco-friendly combustion of the cow dung procedure. The ZnO NPs exhibited a series of diffracted characteristic peaks at 31.8°, 34.4°, 36.3°, 47.5°, 56.6°, 62.8°, 66.5°, 67.9°, and 69.1° which can be assigned to (100), (002), (101), (102), (110), (103), (200), (112), and (201) planes, respectively. All these characteristic reflections are indexed to wurtzite ZnO hexagonal crystalline phase which is well-matched with their standard (JCPDS file no. 36-1451 with space-group *P63mc*, a = 3.243 Å and c = 5.201 Å) (Kumar et al., 2012). The mean crystalline size for the crystal facet of (101) of synthesized ZnO NPs is found to be ~10 nm and the lattice spacing of crystals between the adjacent (101) facets is found to be ~0.25 nm, which are calculated by utilizing the Debye-Scherrer equation and Bragg's law, respectively. Accordingly, the obtained XRD results show the high crystallinity of the prepared material and that no other impurities are detected.

The as-fabricated ZnO NPs is subjected to FTIR spectroscopy analysis Fig. 1(c). The spectral results emphasize the formation of ZnO NPs with an intensive peak below the wavenumber of 500 cm^{-1} belonging to the (Zn–O) stretching vibrations, as previously reported in the literature (Zhu et al., 2010). Nevertheless, the existence of other absorption peaks such as the wide-ranging peak situated at 1064 cm^{-1}, which is attributed to the presence of the absorbed CO_2 probably from the residues of the combustion of cow dung during the synthesis of ZnO NPs (Garba et al., 2019).

The topographic properties of prepared ZnO NPs are examined using FE-SEM. Fig. 2A and B represents the two FE-SEM micrographs for the ZnO NPs in low and high magnifications, respectively. The obtained images of the fabricated ZnO NPs distinctly show the presence of porous on the surface with irregular morphology. The elemental analyses of the fabricated ZnO NPs is con-

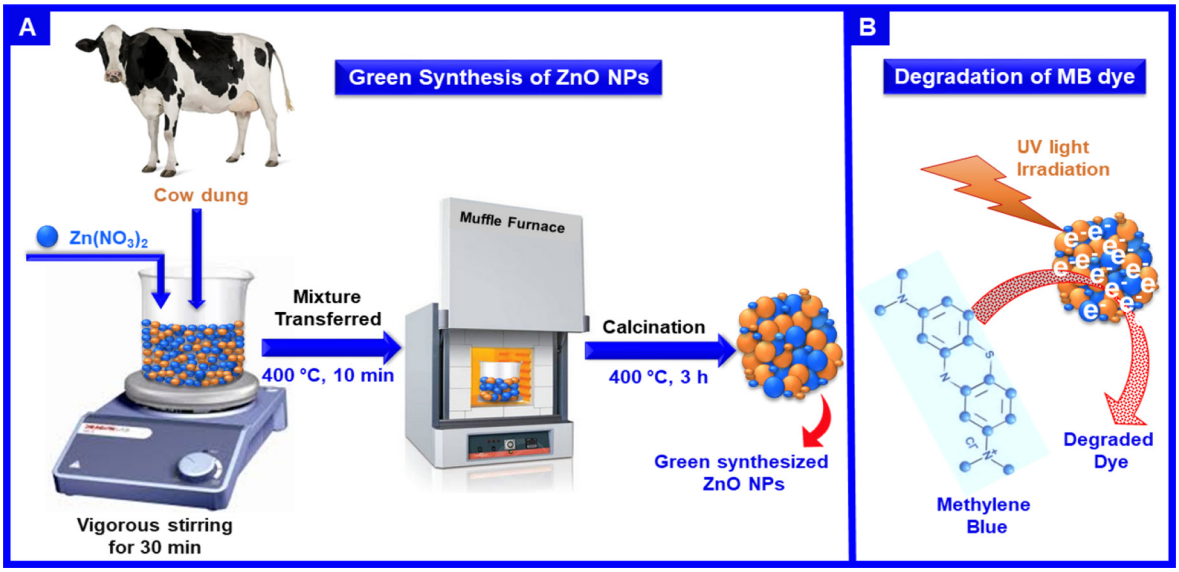

Scheme 1. (A) Scheme illustrating the fabrication of ZnO NPs and (B) Schematic representation of the photodegradation of MB dye.

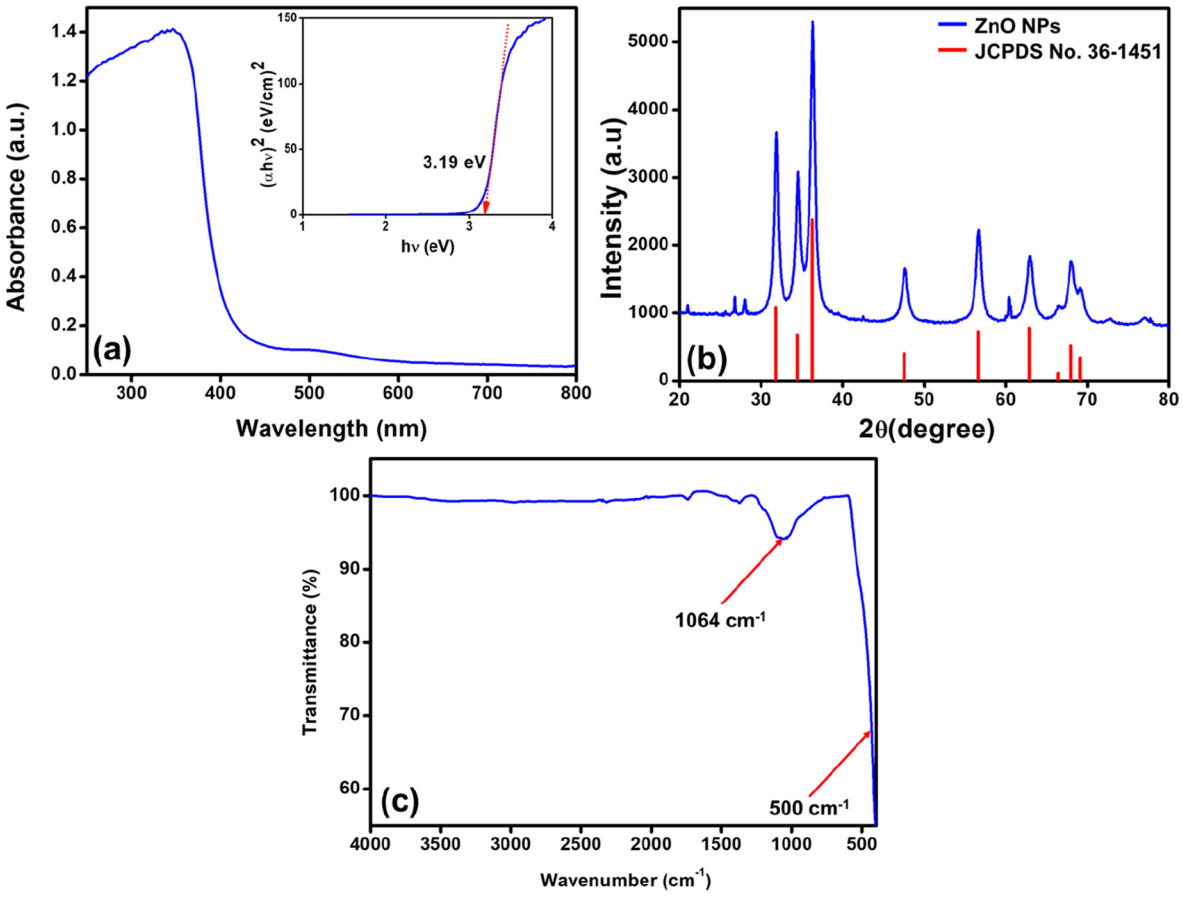

Fig. 1. (a) UV–Vis analysis and bandgap spectra (inset), (b) XRD diffractogram pattern, and (c) FTIR spectra of the fabricated ZnO NPs.

ducted using EDX spectroscopy and the element percentage obtained results is displayed in Fig. 2C. It discloses that the fabricated NPs consists of the desired elements composition i.e. Zn and O, and the elemental composition percentage are illustrated in the internal table.

3.2. Photocatalytic performance results of MB and AZ dyes over ZnO NPs photocatalyst

The main target of this work is to utilize the green synthesized ZnO NPs as photocatalyst for the decomposition of MB and AZ dye

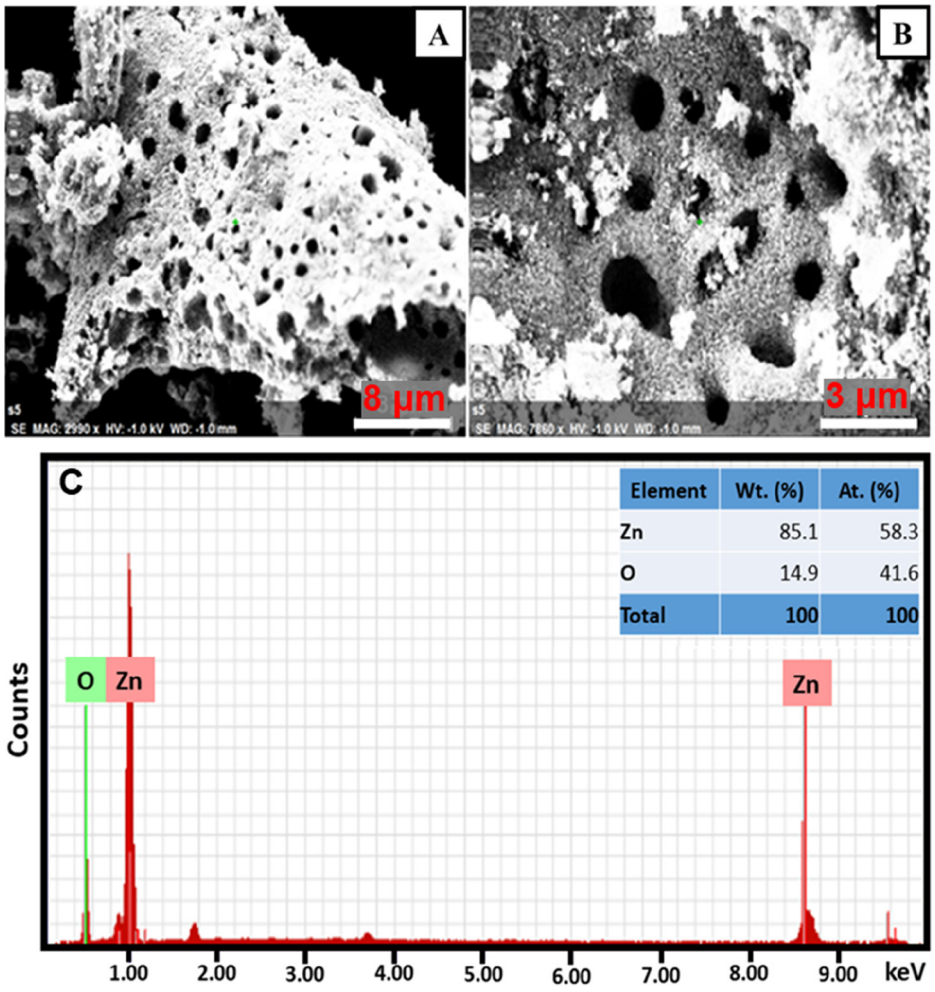

Fig. 2. (A) and (B) FE-SEM micrographs of the fabricated ZnO NPs at different magnification and (C) EDX spectra of the prepared ZnO NPs.

molecules, hazardous chemicals existent in the aqueous effluents from the textile industry. The photocatalytic decomposition efficacy of the fabricated ZnO NPs are tested by changing the various experimental conditions. The theory of semiconductor containing photocatalysts showed that the surface area, bandgap, crystallinity, particle size, morphology, and amounts of free OH· radicals on the photo-catalyst surface determine its photocatalytic activity (Zhang et al., 2018). The theory explained the production of electrons and holes on the photocatalyst surface by the absorption of light and the as-produced electrons and holes will engage in the reaction or undergo recombination. If the extra surface is provided for the electrons and holes, they would relocate where the electrons would be caught by photocatalyst while the holes would be trapped by hydroxyl radicals and generate OH· and HO_2. For metal oxide nanoparticles, more surfaces are available for relocation of photoproduced charge carriers and thus the generated hydroxyl radicals are used effectively to photodegradation of dyes. From the obtained observations from the UV–Vis spectra, it is distinct that the fabricated nanoparticles are active in the UV domain. Additionally, the band-gap is calculated to be E_g = 3.19 eV. The photocatalytic factors including a light source, photocatalyst quantity, concentration of dye, pH value, and irradiation time are systematically examined while MB and AZ are selected as the standard pollutants for photo-catalytic degradation in the report. The difference in absorption intensity of the peak recorded at 663 nm (MB λ_{max}) is monitored to conclude the attained results.

From the absorbance, UV–Vis spectra, C_i and C_f are initial and final dye concentrations of the solution in the photocatalytic system, respectively and the calculation for the degradation activity of the MB and AZ dyes are carried out utilizing the following Eq. (1):

$$\text{Degradation efficacy}\,(\%) = \frac{C_i - C_f}{C_i} \times 100 \quad (1)$$

3.2.1. Influence of light source on dye decomposition

The initial studies are carried out to emphasize the light source that gave the maximum degradation activity of the synthesized ZnO NPs. Therefore, the photocatalytic degradation studies of MB and AZ dyes in the presence of ZnO NPs are conducted in three different conditions i.e. dark, UV light, and visible light. The photocatalytic data obtained are presented in Fig. 3. When the degradation experiment is conducted in the dark, the decomposition of both dyes is insignificant and can be ignored. Besides, when the degradation data obtained from the experiments performed in presence of visible light and UV light are compared, the obtained data revealed that the photodecomposition of MB and AZ dyes under UV light irradiation is considerably higher than the decomposition obtained when visible light is used. For UV light, the prepared ZnO NPs effectively degraded 99.7% of the MB dye which is much higher than visible light, which gave only a 22.0% degradation at a similar irradiation time (100 mins) as displayed in Fig. 3a. Similarly, AZ

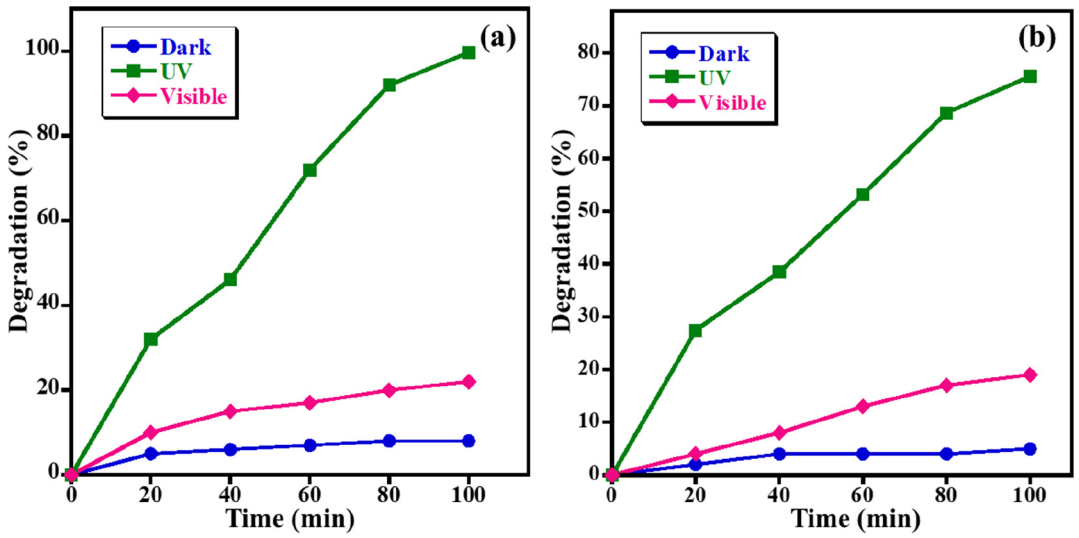

Fig. 3. Effect of light source on photo-catalytic degradation of (a) MB and (b) AZ (Conditions: dye concentration = 5 ppm, photocatalyst amount = 15 mg, and pH of solution = 7).

dye exhibits considerably higher photodegradation activity of 75.6% within 100 mins under UV light compared to visible light, which yielded only 19% degradation of AZ under the same conditions (Fig. 3b). The UV–Vis spectra of the fabricated ZnO NPs supported the results obtained for the photo-decomposition of MB and AZ in presence of UV light. From the above-mentioned observations, it could be stated that the photo-degradation performance of MB and AZ dyes using UV light is better than visible light. Consequently, it could be deduced that the synthesized ZnO NPs is efficient under UV light and all the further optimized studies are conducted under UV light.

3.2.2. Influence of amount of ZnO NPs photocatalyst on dye decomposition

In addition, the optimal photocatalyst dosage for the photodecomposition percentage of MB and AZ dyes is also assessed by altering the quantity of ZnO NPs from 5.0 mg to18.0 mg under UV light irradiation while a 5 ppm dye concentration and pH 7 remained unaltered. The results disclosed that the removal efficacy of both dyes is considerably influenced by the photocatalyst amount (Fig. 4). In the case of MB dye, it is observed that only 65.3% of MB dye degradation when 5.0 mg of photocatalyst is utilized. As expected, when the photocatalyst dose increased to 10.0 mg and 15 mg, 82.6% and 99.9% degradation of MB has detected, respectively. Notwithstanding, further increasing the amount of photocatalyst to 18.0 mg yielded a lower degradation activity and an 88.4% removal percentage of MB is obtained. An identical trend is noticed for the photodecomposition of AZ dye, the degradation activity of AZ dye is also increased linearly with the increase of ZnO NPs photocatalyst. It is obvious that by increasing the catalyst quantity from 5.0 mg to 18.0 mg, a photodegradation of AZ improved from 46.5% to 87.5% at the same photocatalytic conditions (Fig. 4b). This enhancement in the degradation is directly attributed to the introduction of more active sites in the medium that can generate more radical ions. When the photocatalyst dose exceeded a critical boundary there will not be sufficient space for the nanoparticles to disperse in the solution and the particles can stick to each other and become aggregated, owing to the

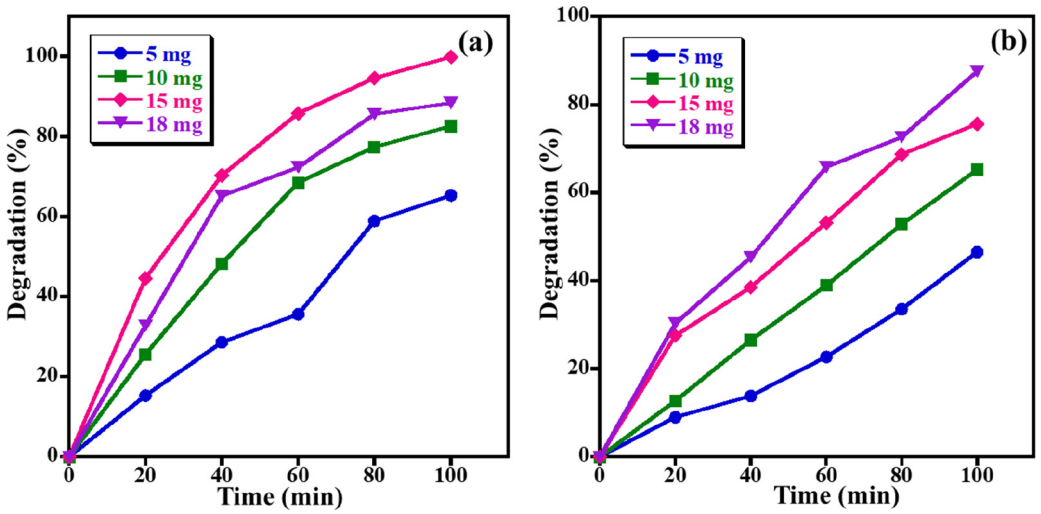

Fig. 4. Impact of quantity of photocatalyst on photo-catalytic decomposition of (a) MB and (b) AZ (Conditions: dye concentration = 5 ppm, pH of solution = 7, and UV light irradiation).

particle's surface energy. Therefore, most of the photocatalytic active sites are blocked or covered up and the degradation efficacy of the system decreased (Nguyen et al., 2018). As illustrated in Fig. 4(a,b), MB shows the best degradation performance at a photocatalyst amount of 15.0 mg, whilst, the highest decomposition of AZ dye at 18.0 mg, nevertheless, the variance of photocatalyst quantity is trivial for MB and AZ dyes. Therefore, 15.0 mg has chosen as the optimal photocatalyst dosage and is utilized for the rest of the experiments to optimize other factors.

3.2.3. Influence of dye concentration on dye decomposition

The impact of dye concentrations on the decomposition performance of the MB and AZ dyes is also assessed by changing the dye concentration from 5.0 ppm to 30.0 ppm using UV light irradiation while maintaining the photocatalyst amount at 15.0 mg and pH 7 as demonstrated in Fig. 5. The obtained results disclosed that the photocatalytic performance of the ZnO NPs is inversely proportional to the concentration of MB and AZ dyes under similar circumstances, i.e. maximum removal efficacy is observed at a minimum concentration (5 ppm). For MB dye, when the MB concentration raised from 5.0 to 30.0 ppm, the MB photodegradation gradually reduced from ~ 99.9% to ~ 87.6%. A similar trend takes place for the degradation of AZ dye, in which the photo-degradation activity of AZ decreased from 75.6% to 39.3% when the AZ concentration increased from 5.0 to 20.0 ppm (Fig. 5b). This abatement owing to the decreased light absorption on the photocatalyst surface by raising the dye concentration, which in turn reduces the production of $OH^{\cdot}$ radical ions which play a vital role in the photodegradation process (Nguyen et al., 2018). Therefore, it is indispensable to keep the ratio of concentration of photocatalysts to dyes alike. As a result, the maximal photodecomposition performance is obtained at the concentration of MB and AZ dyes of 5 ppm, therefore, 5.0 ppm dye concentration has selected in the next optimization studies.

3.2.4. Influence of pH value on dye decomposition

Indeed, the pH value of solution is one of the most important variables in the photocatalytic decomposition of hazardous organic dyes and the photo-catalytic efficacy of the catalyst is commonly linked to the existence of $OH^{\bullet}$ radicals in the reaction medium, which improves the photodegradation of dye numerous folds in basic aqueous solutions. Fig. 6(a,b) discloses the influence of pH solution on photodegradation of MB and AZ dyes in presence of ZnO NPs. The effect of pH of solution on photo-degradation of MB and AZ is studied at four various pH values of 4.0, 5.2, 7.0 and 10.0 with maintaining other variables unaltered (i.e., 5.0 ppm concentration of dye, 15.0 mg catalyst amount and UV light irradiation). The lowest decomposition efficacy is observed at the lowest pH value (i.e., pH 4.0) with 34.3% and 30.6% of MB and AZ being decomposed at 100 min, respectively. Nevertheless, when the pH of the solution raised, the ZnO NPs photocatalyst showed higher degradation activity and 57.3%, 99.7%, and 99.8% degradation of MB are obtained at pH 5.2, 7.0, and 10 (Fig. 6a). This is possibly owing to the higher pH values leading to formation of negative charges on the photocatalyst surface. Since MB is a cationic dye that possesses a positive charge and the dyes have adsorbed on the surface. Additionally, higher amounts of $OH^{\bullet}$ radical ions are adsorbed on the photocatalyst surface and the photodegradation process is carried out more efficiently in higher pH values (Farzana and Meenakshi, 2014). Likewise, the maximal AZ dye degradation activity of 96.8% is achieved at higher pH of 10 under similar conditions as displayed in Fig. 6b. The aforementioned results illustrated that photocatalytic degradation of dye in alkaline medium is considerably higher than acidic medium, which probably ascribed to the enhanced production of $OH^{\cdot}$ radical ions (strong oxidizing species) (Saeed et al., 2016). Similar results were reported by Giacco et al. (2017), which reported that the obtained highest photodegradation of AZ dye at higher pH value due to the oxidation of dye by hydroxyl radicals and positive hole generated in the alkaline medium.

The kinetic studies of photocatalytic degradation of MB and AZ dyes over the synthesized ZnO NPs photocatalyst distinctly displayed that the photocatalytic degradation process occurs through the Langmuir-Hinshelwopseudo-1st-order reaction according to the following Eq. (2):

$$\ln\left(C_i/C_f\right) = kt \tag{2}$$

In the above equation, t (min) is the irradiation time, C_i is the initial dye concentration at t = 0 min, C_f is the final dye concentration at time t, and k is the 1st-order rate constant. The MB pho-

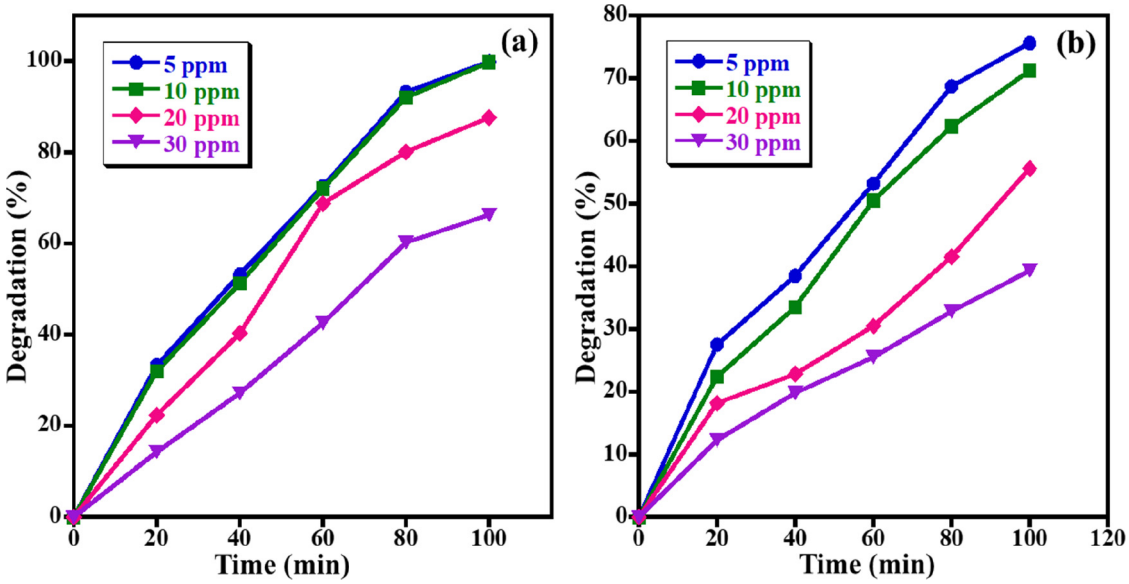

Fig. 5. Effect of initial concentration on photo-catalytic decomposition of (a) MB and (b) AZ. (Conditions: photocatalyst amount = 15 mg, pH of solution = 7, and UV light irradiation).

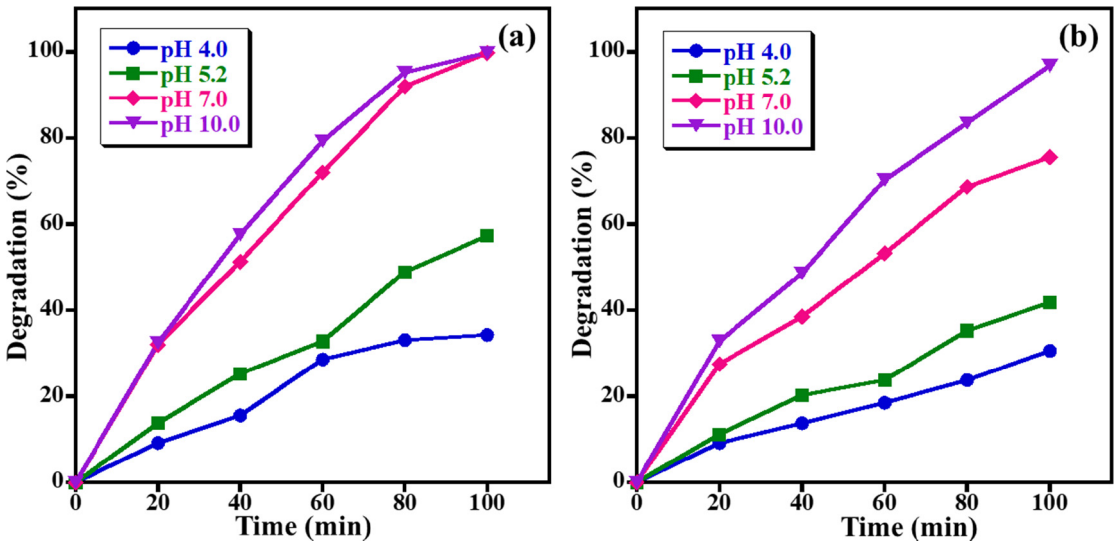

Fig. 6. Effect of pH of solution on photo-catalytic degradation of (a) MB and (b) AZ (Conditions: dye concentration = 5 ppm, photocatalyst amount = 15 mg, and UV light irradiation).

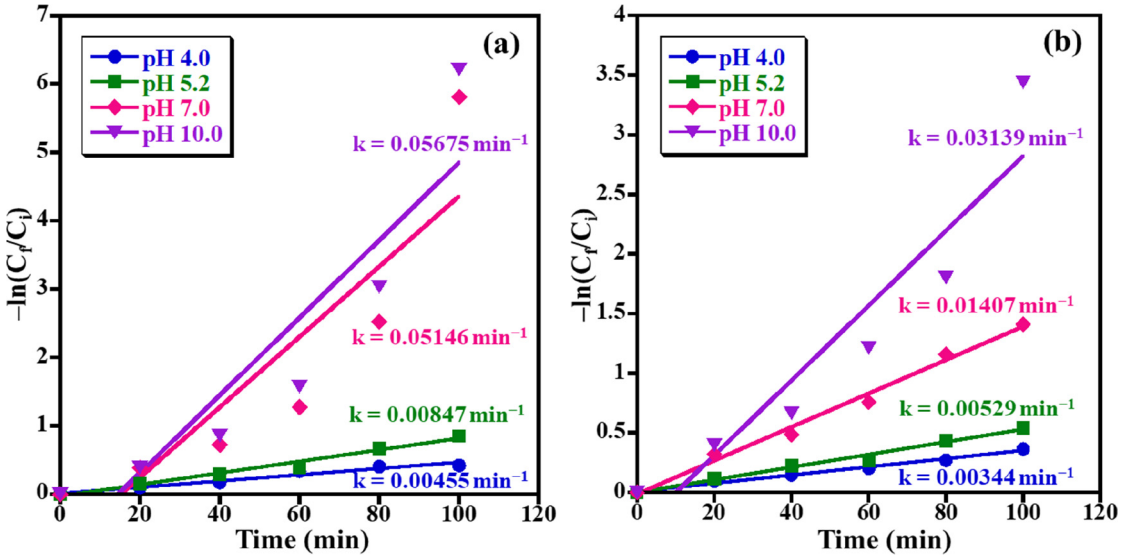

Fig. 7. 1st-order kinetics results for photo-catalytic removal of (a) MB and (b) AZ dyes in presence of ZnO NPs photocatalyst.

todegradation rate constants of 0.00455, 0.00847, 0.05146, and 0.05675 min^{-1} have accomplished for pH 4.0, 5.2, 7.0, and 10.0, respectively (Fig. 7a). Whilst, the MO photodegradation rate constants of 0.00344, 0.00529, 0.01407, and 0.03139 min^{-1} have calculated for pH 4.0, 5.2, 7.0, and 10.0, respectively (Fig. 7b).

A comparison of the photo-decomposition performance of the synthesized ZnO NPs photocatalyst with many formerly photocatalytic systems containing ZnO for removal of MB and AZ, as displayed in Table 1. The prepared ZnO NPs photocatalyst in this study has comparatively superior photo-degradation performance for MB and AZ dyes in using UV light irradiation.

3.3. Photocatalytic mechanism

Scheme 2 illustrates the possible scheme presentation for photocatalytic decomposition of AZ dye on ZnO NPs surface. Under UV light irradiation, the electron-hole pairs are produced between the valence band (VB) and conduction band (CB) of ZnO NPs (Kansal et al., 2013). Therefore, the photo-produced electrons (e^-) generated in the CB of ZnO is scavenged by O_2 to form anion radical ($O_2^{\cdot-}$) which on protonation (H^+) gives HOO·. Nevertheless, the photo-induced holes (h^+) which are generated in the VB of ZnO will react with –OH or H_2O to form very active species of ·OH radical ions. Therefore, the produced ·OH radical ions are responsible for the full mineralization of dye, which in turn produces lower hazardous product such as CO_2 as well as H_2O. Accordingly, the photo-produced •OH and h^+ active species are responsible for the decomposition of harmful pollutant (MB and AZ) dyes, and possible mechanisms can be summed up as follows (Rahman et al., 2013):

$$ZnO + h\nu \rightarrow h^+ + e^- \quad (3)$$

$$e^- + O_2 \rightarrow h^+ + O_2^{\cdot-} \quad (4)$$

$$O_2^{\cdot-} + H^+ \rightarrow h^+ + {}^{\cdot}OOH \quad (5)$$

$$\cdot OOH \rightarrow H_2O_2 + O_2 \quad (6)$$

Table 1
Comparison of photodecomposition efficacy of the current study with other previously published analogues photocatalysts for degradation of MB and AZ dyes.

MB Dye Degradation						
Photocatalyst	Light source	Time (min)	[Dye]	Catalyst dose	Degradation (%)	Ref.
ZnO NPs	UV-lamp	100	5 ppm	15 mg	99.8	Herein
ZnO	Hg-lamp 10 W	120	15 ppm	100 mg	90.0	(Soto-Robles et al., 2021)
Mn-ZnO	UV Lamp	90	10 ppm	24 mg	60.0	(Barick et al., 2010)
ZnO/AC	UV-lamp	45	2×10^{-5} M	0.25 g/L	92.2	(Mydeen et al., 2020)
Ag-ZnO	Solar radiation	30	10 ppm	100 mg	98.5	(Stanley et al., 2021)
Ag-ZnO@GO	Xe-lamp 20 W	180	15 ppm	20 mg	85.0	(Tran Thi et al., 2019)
ZnO/CuO	Solar radiation	120	20 ppm	0.5 g/L	93.0	(Cahino et al., 2019)
AZ Dye Degradation						
ZnO NPs	UV-lamp	100	5 ppm	15 mg	96.8	Herein
ZnO/PNA	UV-lamp 250 W	120	250 ppm	200 mg	85.0	(Riaz et al., 2016)
Cd-ZnS	Solar radiation	120	5×10^{-5} M	30 mg	96.7	(Jabeen, Shah, and Khan 2017)
CuO/ZnO/TiO_2	UV-light 6 W	180	10 ppm	100 mg	100	(Nasief and Abd 2019)
ZnO/GO	Xe-lamp 300 W	90	25 µg/mL	10 µg/mL	95.6	(Anjum et al., 2021)
ZnO SCs	LED lamp 23 W	780	20 ppm	0.1 g	58.0	(Kaur et al., 2020)
30%ZnO/Nylon	UV-light 15 w	300	200 ppm	0.01 g	58.3	(Saeed et al., 2021)

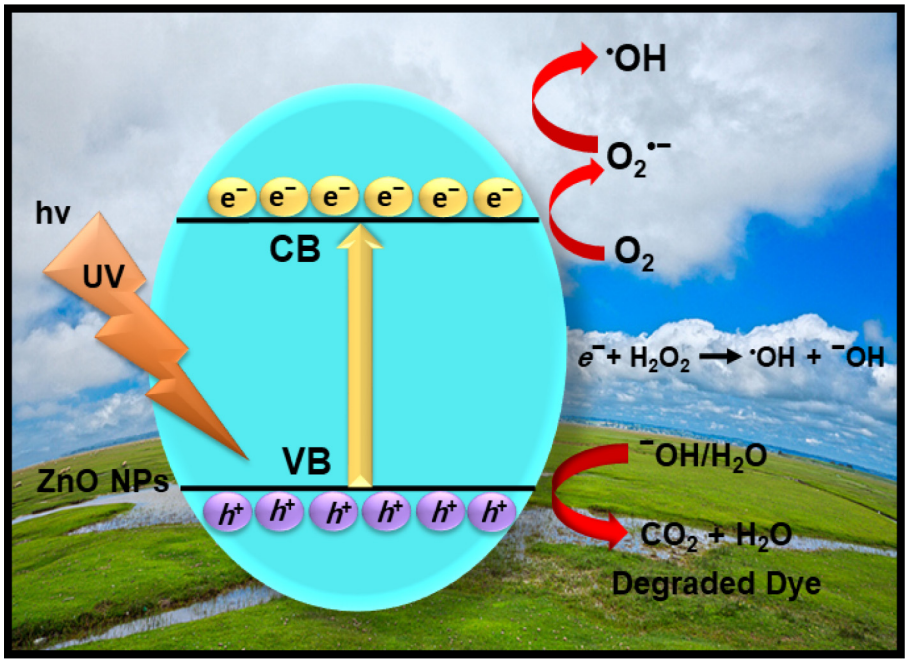

Scheme 2. Possible photo-catalytic mechanism for charge transfer and photodecomposition of MB and AZ over ZnO NPs under UV light irradiation.

$$H_2O_2 + e^- \rightarrow {}^{-}OH + {}^{\bullet}OH \quad (7)$$

$$h^+ + {}^{-}OH/H_2O \rightarrow {}^{\bullet}OH \quad (8)$$

$$^{\bullet}OH + dye \rightarrow Intermediates \rightarrow CO_2 + H_2O \quad (9)$$

According to the aforementioned equations, the photo-decomposition of dye is accomplished over the ZnO NPs photocatalyst.

4. Conclusions

In brief, we report herein the efficacious synthesis of ZnO NPs, using an ecofriendly, facile, and one-pot combustion of cow dung method. The characterizations techniques confirmed the well-crystallinity wurtzite hexagonal ZnO NPs phase. The as-prepared sample is examined as a photo-catalyst for the photodecomposition of MB and AZ dyes, deleterious industrial effluents. The ZnO NPs are used for the photodecomposition of MB and AZ dyes under UV light irradiation, we have found that the fabricated ZnO NPs is efficient and the degradation performance is influenced by the variations in the light source, initial dye concentration, photocatalyst dosage, irradiation time, and pH value of the medium. The highest photocatalytic removal efficacy of MB (99.9%) and AZ (96.8%) was achieved at100 min under the optimal experimental conditions. Hence, it is can be stated that the ZnO NPs act as a highly effective catalyst for the decomposition of MB and AZ dyes which could be ascribed to electron-hole separation produced on the ZnO NPs surface in presence of UV irradiation. Henceforth, the green synthesized ZnO NPs could be employed as a promising candidate for remediation of wastewater and related photocatalytic applications.

Declaration of Competing Interest

The authors declare that they have no known competing financial interests or personal relationships that could have appeared to influence the work reported in this paper.

Acknowledgements

The authors would like to acknowledge the Researchers supporting project number (RSP-2021/222), King Saud University, Riyadh, Saudi Arabia. This work was supported by Vision Group on Science and Technology (SMYSR-2016; GRD 506) Govt. of Karnataka, India, Authors are thankful to the Principal and Management of Don Bosco Institute of Technology for their constant support and Technical Research Centre–Microscopy lab at JNCASR for providing microscopy facilities.

Appendix A. Supplementary data

Supplementary data to this article can be found online at https://doi.org/10.1016/j.jksus.2022.102047.

References

Alharthi, Fahad A., Nabil Al-Zaqri, Adel El marghany, Abdulaziz Ali Alghamdi, Ali Q. Alorabi, Neazar Baghdadi, H. S. Al-Shehri, Rizwan Wahab, and Naushad Ahmad. 2020. 'Synthesis of nanocauliflower ZnO photocatalyst by potato waste and its photocatalytic efficiency against dye', J. Mater. Sci.: Mater. Electron., 31: 11538–11547.

Anjum, F., Asiri, A.M., Khan, M.A., Khan, M.I., Khan, S.B., Akhtar, K., Bakhsh, E.M., Alamry, K.A., Alfifi, S.Y., Chakraborty, S., 2021. Photo-degradation, thermodynamic and kinetic study of carcinogenic dyes via zinc oxide/graphene oxide nanocomposites. J. Mater. Res. Technol. 15, 3171–3191.

Barglik-Chory, C.h., Remenyi, Ch., Strohm, H., Müller, G., 2004. Adjustment of the band gap energies of biostabilized CdS nanoparticles by application of statistical design of experiments. J. Phys. Chem. B 108, 7637–7640.

Barick, K.C., Sarika Singh, M., Aslam, M., Bahadur, D., 2010. Porosity and photocatalytic studies of transition metal doped ZnO nanoclusters. Microporous Mesoporous Mater. 134, 195–202.

Bhushan, B., Jahan, K., Verma, V., Murty, B.S., Mondal, K., 2020. Photodegradation of methylene blue dye by powders of Ni–ZnO floweret consisting of petals of ZnO nanorod around Ni-rich core. Mater. Chem. Phys. 253, 123394.

Cahino, A.M., Loureiro, R.G., Dantas, J., Madeira, V.S., Fernandes, P.C.R., 2019. Characterization and evaluation of ZnO/CuO catalyst in the degradation of methylene blue using solar radiation. Ceram. Int. 45, 13628–13636.

Giacco, D., Tiziana, R.G., Saracino, F., Stradiotto, M., 2017. Counterion effect of cationic surfactants on the oxidative degradation of Alizarin Red-S photocatalysed by TiO2 in aqueous dispersion. J. Photochem. Photobiol., A 332, 546–553.

Farzana, M.H., Meenakshi, S., 2014. Synergistic effect of chitosan and titanium dioxide on the removal of toxic dyes by the photodegradation technique. Ind. Eng. Chem. Res. 53, 55–63.

Garba, J., Samsuri, W.A., Othman, R., Hamdani, M.S.A., 2019. Evaluation of adsorptive characteristics of cow dung and rice husk ash for removal of aqueous glyphosate and aminomethylphoshonic acid. Sci. Rep. 9, 1–10.

Hernández-Carrillo, M.A., Torres-Ricárdez, R., García-Mendoza, M.F., Ramírez-Morales, E., Rojas-Blanco, L., Díaz-Flores, L.L., Sepúlveda-Palacios, G.E., Paraguay-Delgado, F., Pérez-Hernández, G., 2018. Eu-modified ZnO nanoparticles for applications in photocatalysis. Catal. Today.

Jabeen, U., Shah, S.M., Khan, S.U., 2017. Photo catalytic degradation of Alizarin red S using ZnS and cadmium doped ZnS nanoparticles under unfiltered sunlight. Surf. Interfaces 6, 40–49.

Kansal, S.K., Lamba, R., Mehta, S.K., Umar, A., 2013. Photocatalytic degradation of Alizarin Red S using simply synthesized ZnO nanoparticles. Mater. Lett. 106, 385–439.

Kaur, G., Sharma, S., Kaur, K., Bansal, P., 2020. Synthesis, characterization, and visible-light-induced photocatalytic activity of powdered semiconductor oxides of bismuth and zinc toward degradation of Alizarin Red S. Water Environ. Res. 92, 1376–1387.

Koutavarapu, R., Bathula Babu, C.h., Reddy, V., Yoo, K., Cho, M., Shim, J., 2020. A novel one-pot approach of ZnWO 4 nanorods decorated onto gC 3 N 4 nanosheets: 1D/2D heterojunction for enhanced solar-light-driven photocatalytic activity. J. Mater. Sci. 55, 1170–1183.

Kumar, P., Singh, J., Parashar, V., Kedar Singh, R.S., Tiwari, ON.S., Ramam, K., Pandey, A.C., 2012. Investigations on structural, optical and second harmonic generation in solvothermally synthesized pure and Cr-doped ZnO nanoparticles. CrystEngComm 14, 1653–2168.

Look, D.C., 2001. Recent advances in ZnO materials and devices. Mater. Sci. Eng., B 80, 383–437.

López, Uribe, Alvarez Lemus, MC Hidalgo, R López González, P Quintana Owen, S Oros-Ruiz, SA Uribe López, and J Acosta. 2019. 'Synthesis and characterization of ZnO-ZrO2 nanocomposites for photocatalytic degradation and mineralization of phenol', J. Nanomater., 2019.

Maruthupandy, M., Qin, P., Muneeswaran, T., Rajivgandhi, G., Quero, F., Song, J.-M., 2020. Graphene-zinc oxide nanocomposites (G-ZnO NCs): synthesis, characterization and their photocatalytic degradation of dye molecules. Mater. Sci. Eng., B 254, 114516.

Mydeen, S.S., Raj Kumar, R., Sambathkumar, S., Kottaisamy, M., Vasantha, V.S., 2020. Facile synthesis of ZnO/AC nanocomposites using Prosopis Juliflora for enhanced photocatalytic degradation of methylene blue and antibacterial activity. Optik 224, 165426.

Nasief, O.A., Abd, A.N., 2019. Synthesis of nanocomposite and studying the degradation of alizarin dye. J. Biochem. Technol. 10, 69.

Natarajan, S., Bajaj, H.C., Tayade, R.J., 2018a. Recent advances based on the synergetic effect of adsorption for removal of dyes from waste water using photocatalytic process. J. Environ. Sci. 65, 201–222.

Natarajan, T.S., Ravindranathan Thampi, K., Tayade, R.J., 2018b. Visible light driven redox-mediator-free dual semiconductor photocatalytic systems for pollutant degradation and the ambiguity in applying Z-scheme concept. Appl. Catal. B 227, 296–311.

Nguyen, C.H., Chun-Chieh, F.u., Juang, R.-S., 2018. Degradation of methylene blue and methyl orange by palladium-doped TiO2 photocatalysis for water reuse: efficiency and degradation pathways. J. Cleaner Prod. 202, 413–427.

Pouretedal, H.R., Norozi, A., Keshavarz, M.H., Semnani, A., 2009. Nanoparticles of zinc sulfide doped with manganese, nickel and copper as nanophotocatalyst in the degradation of organic dyes. J. Hazard. Mater. 162, 674–681.

Rahman, Q.I., Ahmad, M., Misra, S.K., Lohani, M., 2013. Effective photocatalytic degradation of rhodamine B dye by ZnO nanoparticles. Mater. Lett. 91, 170–214.

Riaz, U., Ashraf, S.M., Budhiraja, V., Aleem, S., Kashyap, J., 2016. Comparative studies of the photocatalytic and microwave–assisted degradation of alizarin red using ZnO/poly (1-naphthylamine) nanohybrids. J. Mol. Liq. 216, 259–267.

Saeed, K., Khan, I., Ahad, M., Shah, T., Sadiq, M., Zada, A., Zada, N., 2021. Preparation of ZnO/Nylon 6/6 nanocomposites, their characterization and application in dye decolorization. Appl. Water Sci. 11, 1–10.

Saeed, K., Khan, I., Sadiq, M., 2016. Synthesis of graphene-supported bimetallic nanoparticles for the sunlight photodegradation of Basic Green 5 dye in aqueous medium. Sep. Sci. Technol. 51, 1421–2146.

Soto-Robles, C.A., Nava, O., Cornejo, L., Lugo-Medina, E., Vilchis-Nestor, A.R., Castro-Beltrán, A., Luque, P.A., 2021. Biosynthesis, characterization and photocatalytic activity of ZnO nanoparticles using extracts of Justicia spicigera for the degradation of methylene blue. J. Mol. Struct. 1225, 129101.

Stanley, R., Alphas Jebasingh, J., Kingston Stanley, P., Ponmani, P., Shekinah, M.E., Vasanthi, J., 2021. Excellent Photocatalytic degradation of Methylene Blue, Rhodamine B and Methyl Orange dyes by Ag-ZnO nanocomposite under natural sunlight irradiation. Optik, 166518.

Subramanian, H., Krishnan, M., Mahalingam, A., 2022. Photocatalytic dye degradation and photoexcited anti-microbial activities of green zinc oxide nanoparticles synthesized via Sargassum muticum extracts. RSC Adv. 12, 985–997.

Suresh, M., Sivasamy, A., 2020. Fabrication of graphene nanosheets decorated by nitrogen-doped ZnO nanoparticles with enhanced visible photocatalytic activity for the degradation of Methylene Blue dye. J. Mol. Liq. 317.

Tran Thi, Viet Ha, Tri Nhut Pham, Tien Thanh Pham, and Manh Cuong Le. 2019. 'Synergistic Adsorption and Photocatalytic Activity under Visible Irradiation Using Ag-ZnO/GO Nanoparticles Derived at Low Temperature', J. Chem., 2019.

Wetchakun, K., Wetchakun, N., Sakulsermsuk, S., 2019. An overview of solar/visible light-driven heterogeneous photocatalysis for water purification: TiO2-and ZnO-based photocatalysts used in suspension photoreactors. J. Ind. Eng. Chem. 71, 19–49.

Zak, A.K., Abrishami, M.E., Majid, W.H.A., Yousefi, R., Hosseini, S.M., 2011. Effects of annealing temperature on some structural and optical properties of ZnO nanoparticles prepared by a modified sol–gel combustion method. Ceram. Int. 37 (1), 393–398.

Zhang, Z., Ma, Y., Xiaohai, B.u., Qiong, W.u., Hang, Z., Dong, Z., Xiaohan, W.u., 2018. Facile one-step synthesis of TiO 2/Ag/SnO 2 ternary heterostructures with enhanced visible light photocatalytic activity. Sci. Rep. 8, 1–11.

Zhu, Q., Chen, J., Zhu, Q., Cui, Y., Liu, L., Li, B.o., Zhou, X., 2010. Monodispersed hollow microsphere of ZnO mesoporous nanopieces: preparation, growth mechanism and photocatalytic performance. Mater. Res. Bull. 45, 2024–2030.